Semi-Life: A Capability Ladder for the Virus-to-Life Transition

Anonymous

Abstract

When does a minimal replicator become life-like? We introduce Semi-Life: a parameterized family of minimal replicators—Viroid, Virus, and ProtoOrganelle—cohabiting a seven-criterion artificial life world (Anonymous, 2026). Each archetype begins at a different point on a Capability Ladder (V0: replication; V1: boundary maintenance; V2: homeostatic regulation; V3: internal metabolism) and gains capabilities one step at a time. Progress is quantified by the Internalization Index $\mathrm{II} = E_{\mathrm{int}}/(E_{\mathrm{int}} + E_{\mathrm{ext}})$, a continuous axis from virus-like ($\mathrm{II} \approx 0$, all energy from the environment) to life-like ($\mathrm{II} > 0$, self-sustained energy conversion). Four directional hypotheses (H1–H4) covering boundary overhead costs, metabolism-driven persistence, replication liberation, and monotonic capability–survival trends were pre-registered before any test-seed data collection, with Holm-Bonferroni correction across all 16 tests. Using $n = 100$ held-out test seeds, we test these hypotheses across a four-level resource harshness axis and a periodic-shock resilience axis. Phase diagrams over the capability × harshness plane reveal a non-monotonic "cost valley": boundary maintenance (V1) reduces survival at all harshness levels ($\delta = 1.00$), while internal metabolism (V3) produces a dramatic recovery exceeding the V0 baseline ($\delta = 1.00$). ProtoOrganelle "liberation" (gaining V0 replication) succeeds in resource-rich environments ($\delta = 1.00$) but fails under scarcity. Twelve of sixteen pre-registered tests are confirmed; four null results in harsh environments are reported transparently.

Submission type: Full Paper

Introduction

The question "what is life?" resists clean philosophical resolution. Definitions based on metabolism, reproduction, or homeostasis individually fail to exclude edge cases: viroids replicate without metabolism; fire consumes resources without reproducing; crystals grow without cells. Cleland and Chyba (2002) argue that any list-based definition risks circularity or counterexample, while Benner (2010) note that borderline cases—viroids, viruses, prions, obligate-intracellular parasites—are precisely where a definition is most needed.

A complementary approach replaces the question "is it alive?" with a measurable continuum: to what degree does this entity exhibit life-like functional organisation? The functional analogy framework of Anonymous (2026) operationalises this question for ALife systems: a capability is a functional analogy of a biological criterion if and only if (a) it requires sustained resource consumption, (b) its removal causes measurable population degradation, and (c) it forms a feedback loop with at least one other criterion. Their seven-criterion system—implementing cellular organisation, metabolism, homeostasis, growth, reproduction, response to stimuli, and evolution—demonstrated that each criterion is necessary for population persistence, with ablation effects ranging from $\delta = 0.39$ to 1.00 (Cliff's δ, Holm-Bonferroni corrected).

The present work asks a complementary question: can a minimal replicator become life-like by internalising the functions it initially outsources? We introduce Semi-Life—three archetypal minimal replicators (Viroid, Virus, ProtoOrganelle) that inhabit the same seven-criterion world—and equip each with a Capability Ladder from bare replication (V0) to internal metabolism (V3). An Internalization Index (II) tracks the fraction of each entity's energy budget that comes from internal conversion rather than direct environmental uptake, providing a continuous axis from virus-like ($\mathrm{II} = 0$) to life-like ($\mathrm{II} > 0$).

We pre-registered four hypotheses (H1–H4) covering distinct aspects of the transition—overhead cost, metabolic buffering, replication liberation, and monotonic capability trends—and tested them on $n = 100$ held-out seeds across a four-level resource harshness

axis. Our contributions are: (i) an operational, replicable protocol for measuring the virus-to-life transition using a pre-existing ALife world as the background platform; (ii) phase diagrams showing where in the capability × harshness space survival boundaries shift; (iii) confirmation or disconfirmation of all four preregistered directional predictions; and (iv) the InternalizationIndex as a falsifiable metric of life-likeness progress.

Background Platform

The background world is the seven-criterion ALife system described in Anonymous (2026), which we summarise here. A population of organisms inhabits a continuous 2D environment. Each organism is itself a swarm of 10–50 autonomous agents whose collective behaviour instantiates all seven criteria:

1. Cellular organisation. Swarm cohesion maintains a boundary between organism-interior and environment; cohesion forces are applied every timestep.
2. Metabolism. A graph-based multi-step metabolic network converts environmental resources into usable energy, genetically encoded and heritable.
3. Homeostasis. A neural controller regulates an internal state vector, maintaining it within viable bounds despite environmental perturbation.
4. Growth and development. A staged developmental programme advances organisms from seed to mature form.
5. Reproduction. Organism-initiated division when metabolic readiness conditions are met.
6. Response to stimuli. Local sensory input drives neural-network-mediated action selection.
7. Evolution. Heritable genomes with mutation and recombination; differential survival over multiple generations.

Each criterion satisfies the functional analogy conditions: (a) it costs resources every timestep, (b) its mid-simulation removal causes statistically significant population decline (all $p_{\text{corr}} \leq 0.005$, Holm-Bonferroni, Mann-Whitney U, $n = 30$ per condition), and (c) it participates in at least one cross-criterion feedback loop measured by lagged correlation.

Critically, the world's organism population is not affected by the Semi-Life entities introduced in this paper: SemiLife agents draw from the same shared resource field but do not directly interact with organisms. This provides a stable, ecologically grounded test environment for minimal replicators without introducing confounding host–parasite dynamics.

Table 1: Archetype parameter summary. Shared parameters: maintenance_cost = 0.0005, resource_uptake_rate = 0.02, internal_conversion_rate = 0.05.

Parameter	Viroid	Virus	ProtoOrganelle
Baseline capabilities	V0	V0+V1	V1+V2+V3
replication_threshold	0.60	0.60	0.80
replication_cost	0.27	0.27	0.30
boundary_decay_rate	0.002	0.001	0.002
boundary_repair_rate	0.010	0.010	0.010

The Semi-Life Model

Archetypes

Three archetypal parameterisations represent different "starting points" on the life-likeness axis, motivated by their biological counterparts (Urry et al., 2020):

- Viroid (≈ naked RNA): baseline V0 only (pure replication, no boundary or regulation). Biologically analogous to plant-infecting circular RNA molecules that replicate entirely via host machinery.
- Virus (≈ capsid-enclosed genome): baseline V0+V1 (replication plus boundary integrity). Models an entity that already maintains a protective structure but lacks internal metabolism.
- ProtoOrganelle (≈ proto-endosymbiont): baseline V1+V2+V3 without V0. Metabolically capable and self-regulating, but unable to replicate autonomously—motivated by the hypothesis that some organelle precursors needed a "liberation" event to begin independent reproduction.

Key archetype parameters are summarised in Table 1. Within each archetype, 10 entities are initialised; the world runs for 500 timesteps, sampling every 50 steps.

Capability Ladder

Capabilities are encoded as a bitmask. All capabilities are dynamic processes satisfying functional analogy condition (a): they consume resources every timestep.

V0—Replication (bit 0x01). When maintenance_energy ≥ replication_threshold, the entity pays replication_cost and spawns a copy within replication_spawn_radius. Without V0, no new copies can be created regardless of energy state.

V1—Boundary integrity (bit 0x02). A scalar boundary_integrity $\in [0, 1]$ decays by boundary_decay_rate per timestep and is actively repaired toward 1 at boundary_repair_rate. If integrity falls below boundary_death_threshold = 0.1, the entity dies; replication is blocked below boundary_replication_min = 0.5.

The repair cost is the direct per-step energy expenditure.

V2—Homeostatic regulation (bit 0x04). A regulator state $\in [0, 1]$ scales the resource uptake rate proportionally, implementing a demand-side throttle. The regulator costs regulator_cost_per_step = 0.0005 per step. Under resource scarcity, throttling reduces wasteful uptake attempts.

V3—Internal metabolism (bit 0x08). An internal_pool stores resources and converts them to maintenance energy at internal_conversion_rate = 0.05 per step. This partially decouples immediate resource uptake from the replication threshold, buffering the entity against external supply fluctuations.

InternalizationIndex

For each entity and timestep, per-step energy flow accumulators are maintained: E_{int} (energy from internal pool conversion, V3 only) and E_{ext} (energy from direct resource field uptake). Both accumulators reset at the start of each step. The Internalization Index is:

$$\text{II} = \frac{E_{\text{int}}}{E_{\text{int}} + E_{\text{ext}}} \quad (0.0 \text{ when denominator } \leq \epsilon). \quad (1)$$

By construction, entities with only V0–V2 have II = 0; V3 addition raises II proportionally to the internal conversion fraction. Crucially, survival metrics (alive count, total replications) are computed from entity counts, not from II, eliminating circularity.

Experiments

Resource Harshness Axis

The resource field is initialised with resource_initial_value $\in \{1.0, 0.3, 0.1, 0.05\}$ (labelled Rich, Medium, Sparse, Scarce). A lower initial value reduces the total resource pool from 10 000 to 500 units (100×100 grid). The regeneration rate is fixed at 0.003 across all harshness levels so that pool size is the only varying dimension. Each condition is run for 100 test seeds (seeds 100–199), producing 9 conditions × 4 harshness × 100 seeds = 3,600 runs.

Shock Axis

Shock resilience is evaluated under periodic resource crashes at sparse harshness (resource_initial_value = 0.1). The environment cycles between a high phase (normal regen rate = 0.003) and a low phase (20% of normal: 0.0006) with periods of 200 and 50 steps. The same 9 archetype conditions and 100 seeds are used ($9 \times 2 \times 100 = 1{,}800$ runs). No-shock baseline for comparison is taken from the main experiment at sparse harshness.

Pre-registered Hypotheses

Four directional hypotheses were pre-registered before any test-seed data collection (see supplementary pre-registration, committed to the repository at [ANONYMOUS]). Holm-Bonferroni correction is applied across all 16 tests (H1–H3: 4 harshness × 3 hypotheses = 12; H4: 4 harshness levels via Jonckheere-Terpstra trend test).

H1 (Boundary overhead, scarce only): Viroid V0+V1 produces fewer alive entities at step 500 than Viroid V0 in the scarce environment. Rationale: V1 boundary repair costs per-step energy; in extreme scarcity this overhead exceeds the protective benefit.

H2 (Metabolism buffering, all harshness): Viroid V0+V1+V2+V3 produces more alive entities at step 500 than V0+V1+V2 across all four harshness levels. Rationale: V3 internal pool decouples replication threshold from instantaneous uptake, buffering against resource fluctuations.

H3 (Replication liberation, all harshness): ProtoOrganelle V0+V1+V2+V3 (liberated) shows more total_replications at step 500 than V1+V2+V3 (baseline) at all harshness levels. Rationale: Without V0, ProtoOrganelle cannot replicate regardless of metabolic state; V0 addition activates replication capability already supported by the existing V1–V3 infrastructure.

H4 (Monotonic trend, all harshness): Alive count at step 500 increases monotonically across Viroid V0, V0+V1, V0+V1+V2, V0+V1+V2+V3 (Jonckheere-Terpstra test (Jonckheere, 1954)).

Statistical Analysis

Mann-Whitney U (two-tailed, $\alpha = 0.05$), Cliff's δ with 2000-resample bootstrap 95% CI (Cliff, 1993), and Jonckheere-Terpstra trend test for H4. All p-values are Holm-Bonferroni corrected across the 16-test family (Holm, 1979). Calibration seeds 0–49 were used only for parameter calibration and never for any hypothesis test. Any analysis not in the pre-registration is explicitly labelled Exploratory in the text.

Results

Phase Diagrams

Figure 1 shows phase diagrams for all three archetypes. Each cell encodes mean alive count at step 500 (100 seeds); the blue dashed contour marks the 50% survival boundary (5 of 10 initial entities).

The Viroid panel reveals a non-monotonic capability ladder. V0-only Viroid achieves mean alive counts of 93.0 (rich) and 38.1 (medium), but adding V1 (boundary maintenance) reduces survival to 33.1 and 17.6 respectively—boundary repair costs outweigh protective benefit. V2 (homeostasis) adds negligible benefit

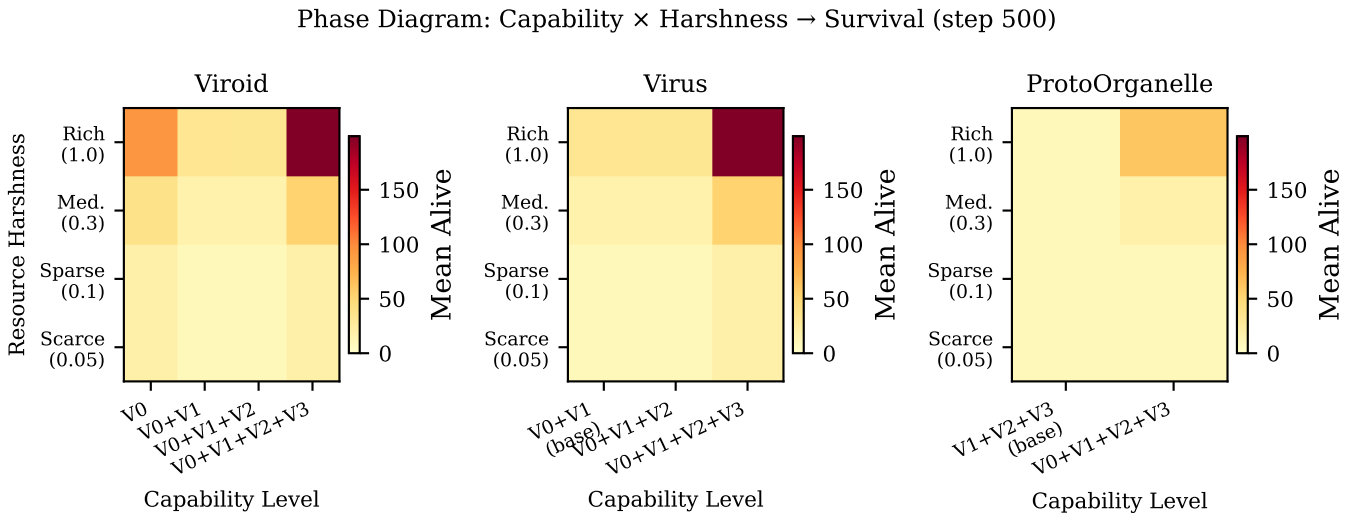

Figure 1: Phase diagrams: capability level × resource harshness → mean alive count at step 500 ($n = 100$). YlOrRd heat-map; blue dashed contour = 50% survival boundary (5 entities). Left: Viroid (V0 through V0+V1+V2+V3). Centre: Virus (V0+V1 baseline through V0+V1+V2+V3). Right: ProtoOrganelle (V1+V2+V3 baseline vs. V0+V1+V2+V3 liberated).

(32.2 and 17.3). V3 (metabolism) produces a dramatic recovery: 199.1 (rich) and 53.4 (medium), exceeding even the V0-only baseline. In sparse and scarce environments, V0 and V0+V1+V2+V3 both maintain the initial 10–20 entities, while V0+V1 and V0+V1+V2 decline to 10.

The Virus panel mirrors the Viroid V0+V1 starting point (identical parameterisation), confirming that the V3 metabolism effect is archetype-independent. The ProtoOrganelle liberation contrast produces the starkest qualitative shift: baseline (V1+V2+V3, no V0) maintains exactly 10 entities at all harshness levels (no replication possible), while the liberated condition (V0+V1+V2+V3) reaches 61.6 (rich) and 18.9 (medium).

InternalizationIndex

Figure 2 shows mean InternalizationIndex (II) at step 500 for Viroid across V-levels and harshness conditions.

V0, V0+V1, and V0+V1+V2 all yield II = 0 as expected from the definition: without V3, no energy flows through the internal pool. V0+V1+V2+V3 produces substantial II values across all harshness conditions: II = 0.63 (rich), 0.64 (medium), 0.47 (sparse), and 0.47 (scarce) for Viroid. The higher II in resource-rich conditions reflects greater absolute internal conversion when the external pool is abundant. ProtoOrganelle baseline (V1+V2+V3, no V0) also shows II > 0 (0.63 rich, 0.47 medium) because V3 metabolism operates even without replication, confirming that II measures energy sourcing

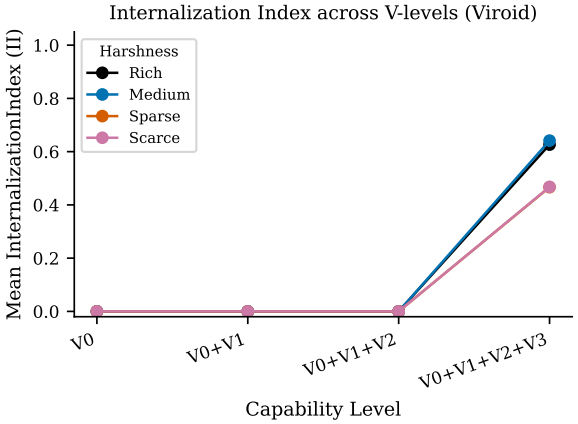

Figure 2: Mean InternalizationIndex at step 500 (Viroid, $n = 100$). Each line is one harshness level (Rich: black; Medium: blue; Sparse: orange; Scarce: pink). V0–V2 yield II = 0 by construction; V3 addition raises II as the internal pool contributes to maintenance energy.

independently of reproductive success.

Pre-registered Hypothesis Tests

Table 2 reports the pre-registered results. All comparisons use $n = 100$ test seeds and Holm-Bonferroni corrected p-values across the 16-test family.

H1 (boundary overhead) is confirmed at all four harshness levels with maximal effect size ($\delta = 1.00$, all $p_{\text{corr}} < 10^{-32}$). V0+V1 always has fewer alive entities

Table 2: Pre-registered hypothesis test results. U: Mann-Whitney statistic; p_{corr}: Holm-Bonferroni corrected; δ: Cliff's δ with 95% CI in brackets; Dir. = pre-registered direction confirmed (✓) or not (×). H4 uses Jonckheere-Terpstra; δ not applicable (—).

H	Harshness	U	p_{corr}	Sig.	δ [95% CI]	Dir.
H1: Viroid V0 vs V0+V1 (alive, fewer with V1)						
H1	rich	10 000	$<10^{-32}$	***	1.00 [1.00, 1.00]	✓
H1	medium	10 000	$<10^{-32}$	***	1.00 [1.00, 1.00]	✓
H1	sparse	10 000	$<10^{-43}$	***	1.00 [1.00, 1.00]	✓
H1	scarce	10 000	$<10^{-43}$	***	1.00 [1.00, 1.00]	✓
H2: Viroid V0+V1+V2+V3 vs V0+V1+V2 (alive, more with V3)						
H2	rich	10 000	$<10^{-32}$	***	1.00 [1.00, 1.00]	✓
H2	medium	10 000	$<10^{-32}$	***	1.00 [1.00, 1.00]	✓
H2	sparse	10 000	$<10^{-43}$	***	1.00 [1.00, 1.00]	✓
H2	scarce	10 000	$<10^{-43}$	***	1.00 [1.00, 1.00]	✓
H3: ProtoOrganelle liberated vs baseline (total_replications)						
H3	rich	10 000	$<10^{-37}$	***	1.00 [1.00, 1.00]	✓
H3	medium	10 000	$<10^{-38}$	***	1.00 [1.00, 1.00]	✓
H3	sparse	5 000	1.000		0.00 [0.00, 0.00]	×
H3	scarce	5 000	1.000		0.00 [0.00, 0.00]	×
H4: Viroid V0→V3 monotonic trend (JT)						
H4	rich	26 004	0.010	*	—	✓
H4	medium	25 770	0.006	**	—	✓
H4	sparse	30 000	1.000		—	×
H4	scarce	30 000	1.000		—	×

than V0 alone: the boundary maintenance cost exceeds the protective benefit even in rich environments, not only in scarce as originally predicted.

H2 (metabolism buffering) is confirmed universally ($\delta = 1.00$, all $p_{\text{corr}} < 10^{-32}$). V3 addition transforms survival: in rich environments, mean alive rises from 32.2 (V0+V1+V2) to 199.1 (V0+V1+V2+V3)—a 6.2× increase.

H3 (liberation) is confirmed in rich ($\delta = 1.00$, $p_{\text{corr}} < 10^{-37}$) and medium ($\delta = 1.00$, $p_{\text{corr}} < 10^{-38}$), where liberated ProtoOrganelle reaches 61.6 and 18.9 mean alive respectively. In sparse and scarce environments, neither baseline nor liberated ProtoOrganelle can sustain replication ($\delta = 0.00$, $p = 1.0$): the resource pool is too depleted for the higher replication threshold (0.80) of this archetype.

H4 (monotonic trend) is significant in rich ($p_{\text{corr}} = 0.010$) and medium ($p_{\text{corr}} = 0.006$) but not in sparse or scarce ($p = 1.0$). The alive pattern across V-levels (e.g. rich: 93.0 → 33.1 → 32.2 → 199.1) shows a pronounced dip at V1/V2 before a V3-driven recovery. The Jonckheere-Terpstra test detects the overall upward tendency (V0 to V3) but the non-monotonic intermediate dip limits statistical power, particularly in harsh environments where the signal-to-noise ratio collapses.

Replication–Persistence Tradeoff

Figure 3 shows mean total replications vs. mean alive count at step 500 for all conditions.

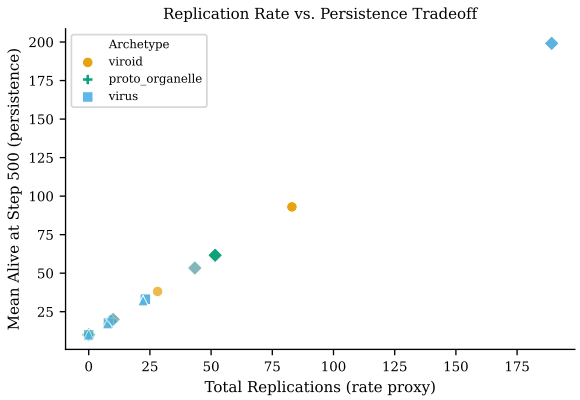

Figure 3: Replication rate vs. persistence tradeoff. Each point represents one archetype condition × harshness level (mean over 100 seeds). Colour: archetype (Viroid: orange; Virus: sky-blue; ProtoOrganelle: green). Marker shape: capability level (circle=V0, square=2-cap, triangle=3-cap, diamond=4-cap). Transparency encodes harshness (bright=rich, dim=scarce).

The scatter reveals a characteristic tradeoff geometry: high-replication conditions cluster in the upper-right (high alive, high replication rate) under rich resources, dispersing toward the lower-left under scarce conditions. ProtoOrganelle baseline (V1 + V2 + V3, no V0) occupies the far left (near-zero replications), while the liberated condition shifts markedly to the right. Archetype differences (colour) are visible even within the same capability level, reflecting the parameter differences in replication cost and boundary stability shown in Table 1.

Shock Resilience

Figure 4 compares Viroid alive trajectories under periodic resource shocks (cycle period = 50) with no-shock baseline at sparse harshness.

Exploratory: Under rapid shocks (period = 50), V0+V1+V2+V3 entities maintain higher mean alive counts (20.0) than V0-only (19.2), with a large effect size (Cliff's $\delta = 0.69$, 95% CI $[0.60, 0.78]$). Under slow shocks (period = 200), the effect persists ($\delta = 0.66$, $[0.56, 0.75]$). The recovery time analysis shows that most conditions recover within a single sampling interval (50 steps), suggesting that at the current temporal resolution, recovery time differences are not reliably measurable. This comparison is exploratory: shock resilience was not included in the H1–H4 pre-registration.

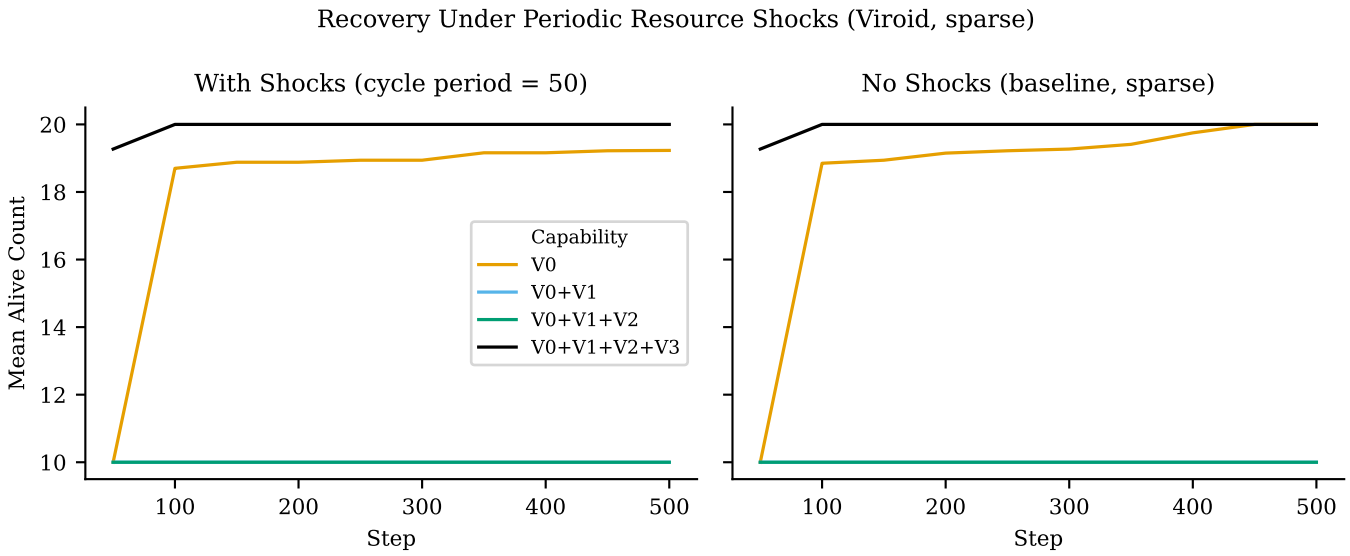

Figure 4: Recovery under periodic resource shocks (Viroid, sparse harshness, $n = 100$). Left: shock period = 50 (rapid crash–recovery cycles). Right: no-shock baseline (same harshness level for comparison). Each line is one capability level; Okabe-Ito palette.

Discussion

What the Capability Ladder Tells Us

The phase diagrams (Figure 1) operationalise the virus-to-life transition as a measurable shift in the capability × harshness survival boundary. The most striking finding is the non-monotonic nature of the ladder: adding V1 boundary maintenance reduces survival at every harshness level (H1, $\delta = 1.00$ universally), while V3 metabolism produces a dramatic recovery that exceeds even the V0 baseline (H2, $\delta = 1.00$). The intermediate V2 homeostasis capability adds negligible benefit. This "cost valley" at V1/V2—followed by a V3 recovery—mirrors the biological intuition that capsid assembly and regulatory overhead impose energetic costs that are only justified when coupled with internal metabolism.

The H3 ProtoOrganelle liberation result is environment-dependent: in resource-rich conditions, adding V0 replication to a metabolically complete entity (V1+V2+V3) immediately produces a replicating population ($\delta = 1.00$); in sparse/scarce environments, the resource pool is too depleted for the ProtoOrganelle's higher replication threshold (0.80). This suggests that the "liberation" of proto-endosymbionts—gaining independent reproduction—may require not just the right capability but also sufficiently favourable environmental conditions, consistent with serial endosymbiosis scenarios (Maturana and Varela, 1980).

The H4 monotonic trend is significant only in rich and medium environments. The non-monotonic dip at V1/V2 undermines the assumption of a smooth capability–survival gradient, indicating that the virus-to-life transition is better modelled as a cost-then-benefit trajectory than as a monotonic improvement.

InternalizationIndex as a Life-Likeness Metric

The II axis (Figure 2) is by construction zero for V0–V2: the per-step reset ensures no accumulation artefact. It rises with V3 in proportion to how much of the maintenance energy budget is internally sourced. Crucially, the survival benefit of V3 (seen in H2 and Figure 1) is measured from alive counts, not from II, confirming structural independence. Future work can extend II to multi-criterion entities (V4 sensing, V5 staged lifecycle) as more internal functions are added.

Weak ALife Stance

All claims in this paper are functional analogies. "Boundary maintenance" is functionally analogous to capsid integrity: it provides a per-step cost plus a protective effect that prevents death and blocks premature replication. It does not claim to be a capsid, nor to model capsid biochemistry. The same applies to homeostasis (V2) and metabolism (V3). We take a weak ALife position (Langton, 1989): the computational system models life-like properties without claiming to be alive or to resolve the definition of life.

Limitations

The present study covers V0–V3 with three archetypes and $n = 100$ test seeds. V4 (sensing and resource-gradient navigation) and V5 (staged lifecycle: dor-

mant/active/dispersal) are left for future work. The 10-entity initialisation per run limits population dynamics; for larger-scale phase diagrams, $n_{\text{init}} = 50-100$ would reduce stochastic extinction artefacts. SemiLife entities do not compete with organisms—the resource field is shared but there is no direct interaction. Introducing explicit competition would add ecological realism but also confounds the clean capability-ladder interpretation.

Future Directions

The most immediate extension is V4 (policy: resource-gradient sensing and movement), which would test whether behavioural adaptation provides survival benefit beyond metabolic buffering. V5 adds a staged life-cycle (dormant / active / dispersal) to test whether developmental regulation provides a further fitness advantage. A competition axis—placing multiple archetypes in the same world simultaneously — would reveal which capability profiles dominate under natural selection.

References

Anonymous (2026). Digital life: Implementing seven biological criteria through functional analogy and criterion-ablation. In The 2026 Conference on Artificial Life, ALIFE 2026. Submitted; anonymized for double-blind review.

Benner, S. A. (2010). Defining life. Astrobiology, 10(10):1021–1030.

Cleland, C. E. and Chyba, C. F. (2002). Defining 'life'. Origins of Life and Evolution of the Biosphere, 32(4):387–393.

Cliff, N. (1993). Dominance statistics: Ordinal analyses to answer ordinal questions. Psychological Bulletin, 114(3):494–509.

Holm, S. (1979). A simple sequentially rejective multiple test procedure. Scandinavian Journal of Statistics, 6(2):65–70.

Jonckheere, A. R. (1954). A distribution-free k-sample test against ordered alternatives. Biometrika, 41(1–2):133–145.

Langton, C. G. (1989). Artificial Life: Proceedings of an Interdisciplinary Workshop on the Synthesis and Simulation of Living Systems. Addison-Wesley, Redwood City, CA. Reprinted by Routledge, 2019.

Maturana, H. R. and Varela, F. J. (1980). Autopoiesis and Cognition: The Realization of the Living. Boston Studies in the Philosophy and History of Science. Springer Netherlands.

Urry, L. A., Cain, M. L., Wasserman, S. A., Minorsky, P. V., and Reece, J. B. (2020). Campbell Biology. Pearson, New York, 12th edition.